A highly efficient *in situ* redox stabilization strategy for Am-Cm separation using $AgBiO_3$

Parveen K. Verma[a], Arunasis Bhattacharyya*[,a], Soumen Samanta[b], Prasanta K. Mohapatra*[,a]

[a] Radiochemistry Division, [b] Technical Physics Division

[a.] *Radiochemistry Division, Bhabha Atomic Research Centre, Trombay, Mumbai-400085, India. *Corresponding Authors, E-mail: arun12@barc.gov.in(AB), mpatra@barc.gov.in(PKM)*
[b.] *Technical Physics Division, Bhabha Atomic Research Centre, Trombay, Mumbai-400085, India*

Contents

List of Tables

List of Figures

Introduction

There are reports on Am-Cm/Eu separations by oxidizing Am^{3+} to AmO_2^+ using $Na_2S_2O_8$ along with hypochlorite[1] and Ag^+ salts.[2] Burns et al, reported SFs of 30 (±10)[1] and 60 (±20)[3] and 20[4] for AmO_2^+/Nd^{3+}, AmO_2^+/Eu^{3+} and AmO_2^+/Cm^{3+} using Na–Sn–hybrid, respectively, followed by Am^{3+} oxidation to AmO_2^+ at pH~2 (HNO_3). The average SF (Cm/Am) of 110±20 was reported by Kazi et al.,[2] for Am-Cm separation using the DGA resin followed by Am^{3+} oxidation to AmO_2^+ at pH 2 (HNO_3). Very high SF ($>10^4$) for Am-Eu and Am-Cm separation was reported by oxidizing Am^{3+} to AmO_2^+ in the organic medium using $HBiO_3$ extracted with the DGA ligand by adduct formation.[5-7] The same group has also reported a SF of $>10^5$ for americium/lanthanides separation using a biphasic system.[5] The oxidation achieved in these studies involved the organic phase which appeared less complex as compared to the aqueous phase which contained various complexing ions.

Am^{3+} can be oxidized to AmO_2^{2+} using several regents under different chemical conditions.[8-13] For example, using $NaBiO_3$ in nitric acid,[9] O_3 in carbonate solution,[14] $Na_2S_2O_8$ at 80°C in slightly acidic solutions,[15], etc.[8] Contrary to these, only a few methods are reported for the direct oxidation of Am^{3+} to AmO_2^+ and are predominantly formed in circumneutral and alkaline conditions.[8] Few common oxidizing agents are ozone, peroxydisulfate[1, 4], or hypochlorite[16] for the direct oxidation of Am^{3+} to AmO_2^+.[8] The auto reduction of AmO_2^{2+} also leads to the *in-situ* formation of AmO_2^+.[17, 18]

The $Am^{3+} \rightarrow AmO_2^+$ oxidation by $NaBiO_3$ under heating conditions was suggested by Mincher et al.[9] However, Burns et al,[1] have not succeeded in the preparation of AmO_2^+ by this method[9] and used $Na_2S_2O_8$, instead for oxidation.[1] The same group also reported the formation of AmO_2^+ and AmO_2^{2+} from the Am^{3+} oxidation by sulfate radical oxidation in HNO_3 and $HClO_4$ medium, respectively.[4] The addition of excess hypochlorite ions is a prerequisite to stabilize and maintain the AmO_2^+ state in both HNO_3 and $HClO_4$ medium and Am-Cm separation was shown.[4] Later, Mincher et al.,[19] optimized the procedure given by Burns et al.,[4] and achieved quantitative oxidation of Am^{3+} to AmO_2^+ in 0.1 M HNO_3 with 1.0 M $Na_2S_2O_8$ at 80-100 °C. Although, the $Na_2S_2O_8$-based methods for the generation of AmO_2^+ are promising but require heating at elevated temperatures for 10-45 minutes.[4] The added $Na_2S_2O_8$ also leads to the generation of secondary wastes along with an *in situ* generation of SO_4^{2-} ions along with $S_2O_8^{2-}$, OCl^-, as well as ClO_x^-

(generated by decomposition of the $Ca(OCl)_2$)and $CaSO_4$ precipitation[4] making the overall process complicated.

The AmO_2^+ generation by the $NaBiO_3$ mediated oxidation of Am^{3+} under heating conditions is cleaner[9] but introduces Bi^{3+} ions into the solution due to the dissolution of $NaBiO_3$ followed by its rapid reduction in acidic solution at the temperature used to achieve the $Am^{3+} \rightarrow AmO_2^+$ conversion. The other methods employ high carbonate concentration[14, 20] and also lead to the formation of the AmO_2^+-carbonate complex rather than the pure hydrated AmO_2^+ ions.

Rice, et al.,[21] have recently used $NaBiO_3$ as an oxidant and reported the formation of AmO_2^+ in HCl at pH 1. However, HCl is not only corrosive but its addition to $NaBiO_3$ leads to Cl_2 evolution[22] along with the formation of BiOCl precipitates[22] making the process complicated if applied for Am separation beside the loss of $NaBiO_3$.

$AgBiO_3$ characterization

X-ray diffraction and XPS analysis

The XRD data of the $NaBiO_3$ used in the present study matched well with the JCPDF file number PDF # 30-1161, suggesting the di-hydatre form of the $NaBiO_3$ i.e. ($NaBiO_3.2H_2O$) used in the present studies.[23] XRD of $AgBiO_3$ (dried at room temperature) prepared at different AgNO3: NaBIO3 mole ratio was recorded using XRD unit from Rikagu, Japan. The XRD shows similar pattern for1:1 to 1:3 mole ratio of $NaBiO_3$:$AgNO_3$, suggesting that even 1:1 mole ratio is enough for ion exchange of Na^+ with Ag^+ to form $AgBiO_3$. X-ray photoelectron spectroscopy (XPS) measurement of the $AgBiO_3$ was carried out using DESA-150 electron analyzer (Staib Instruments, Germany) and Mg-Ka (1253.6 eV) source. The binding-energy was calibrated using Au-$4f_{7/2}$ line with energy 84.0 eV and C-1s line of energy 284.8 eV. The deconvolution of high-resolution peaks was carried out using XPSPEAK4.1 software.

Am-Eu and Am-Cm separation

The known volume of the Am+Eu mixture was taken at pH 4 and its initial activity was counted using HpGe detector. The mixture was equilibrated with different amount of $AgBiO_3$ for 5, 30 and

60 minutes. The resultant suspension was centrifuged at 7000g for 10 minutes and the small aliquot (~100 µl) from supernatant was counted using HpGe detector. The similar procedure was used for Am-Cm separation. The initial sample and supernatant after $AgBiO_3$ treatment was analyzed using α-spectrometry.

Figures and Tables

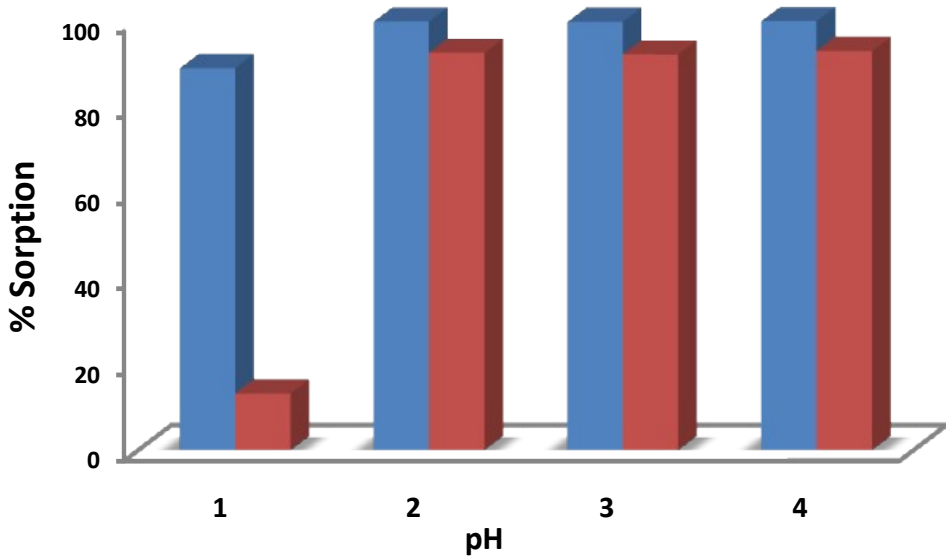

Figure S1. The sorption of Eu^{3+} (blue bar) and Am^{3+}(red bar) onto $NaBiO_3$ at different pH, Time: 5 minutes, $[Am^{3+}] = [Eu^{3+}]$: 1×10^{-6} M, $[NaBiO_3]$: 2.5 mg/mL, Temperature: 25 °C, (The initial and final counts of radiotracer in sorption studies were determined using NaI(Tl) detector.)

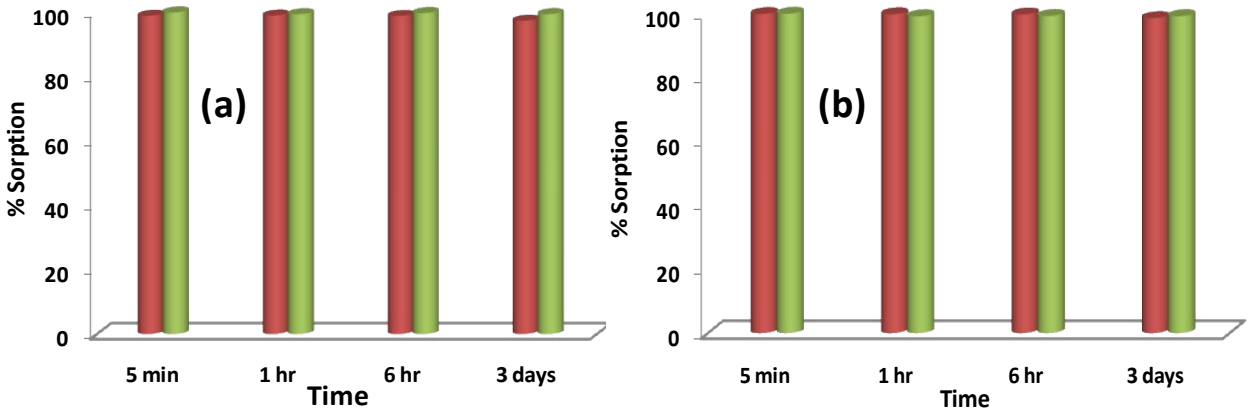

Figure S2. The sorption of Eu^{3+}(red bar) and Am^{3+}(green bar) onto $NaBiO_3$ at pH~4 at different time interval for (a) $NaBiO_3$ and (b) H^+-$NaBiO_3$, [Am^{3+}] = [Eu^{3+}]: 1×10^{-6} M, [$NaBiO_3$]: 2.5 mg/mL, pH : 4, Temperature: 25 °C, (The initial and final counts of pure radiotracer in sorption studies were determined using NaI(Tl) detector.).

Eh-pH or Pourbaix diagram

The Pourbaix diagram gives the thermodynamic stability field for different oxidation states of Am in the presence of BiO_3^-→Bi^{3+} couple under different pH conditions (the hydrolysis of Am^{3+} not included and plotted separately for better representation). The equation used for the Pourbaix diagram is given in Table S1. Although, the higher oxidation stats of the Am occurs above the stability line of water oxidation (H_2O→O_2) but thermodynamic conditions for Am^{3+}→AmO_2^+ or Am^{3+}→AmO_2^{2+} can be inferred from these diagrams. The Am^{3+} is the only stable species in the absence of any complexing agents, rest all the higher oxidation states of Am prefer to reduce to Am^{3+} by oxidizing water to oxygen. The Eh-pH diagram suggest the AmO_2^+ formation is difficult below pH 1.5 using BiO3→Bi^{3+} couple and prefer to go to the AmO_2^{2+} state. The marked stability field for AmO_2^+ is narrow and even beyond pH 6 (Fig. S3). The equation used for the speciation plot is given in Table S2, the BiO_3^-→Bi^{3+} couple crosses the Am^{3+}→AmO_2^+ lines suggesting its poor oxidation ability beyond that point and hence one has to limit the pH range between pH 1.5 to 6 to achieve Am^{3+}→AmO_2^+ conversion using BiO_3^-→Bi^{3+} couple. However, the higher pH (>5) causes formation of the Am-hydroxo species and lower pH (<3) further narrow the stability field and also increase the tendency of disproportionation of AmO_2^+ formed by Am^{3+} oxidation. This

made us to choose pH ~4 as a safe range for getting stable AmO_2^+. The Ag^{2+} and S_2O_8 have very high potential and can oxidize Am^{3+} to AmO_2^{2+} under in entire pH range (assuming no other side reaction).

Table S 1. Half cell reaction used to generate Pourbaix diagram of Am,Ag, $S_2O_8^{2-}$, and BiO_3^- system.

Couple	**Equations**	**Standard reduction potential, E^0 (V) (I= 0))**
$AmO_2^+ \rightarrow Am^{3+}$	$AmO_2^+ + 4H^+ + 2e^- \rightarrow Am^{3+} + 2H_2O$	1.75[24]
$AmO_2^{2+} \rightarrow Am^{3+}$	$AmO_2^{2+} + 4H^+ + 3e^- \rightarrow Am^{3+} + 2H_2O$	1.70[24]
$AmO_2^{2+} \rightarrow AmO_2^+$	$AmO_2^{2+} + e^- \rightarrow AmO_2^+$	1.60[24]
$BiO_3^- \rightarrow Bi^{3+}$	$BiO_3^- + 6H^+ + 2e^- \rightarrow Bi^{3+} + 3H_2O$	2.03[25]
$Ag^{2+} \rightarrow Ag^+$	$Ag^{2+} + e^- \rightarrow Ag^+$	1.98[3]
$S_2O_8^{2-} \rightarrow SO_4^{2-}$	$S_2O_8^{2-} + 2e^- \rightarrow 2SO_4^{2-}$	2.01[8]

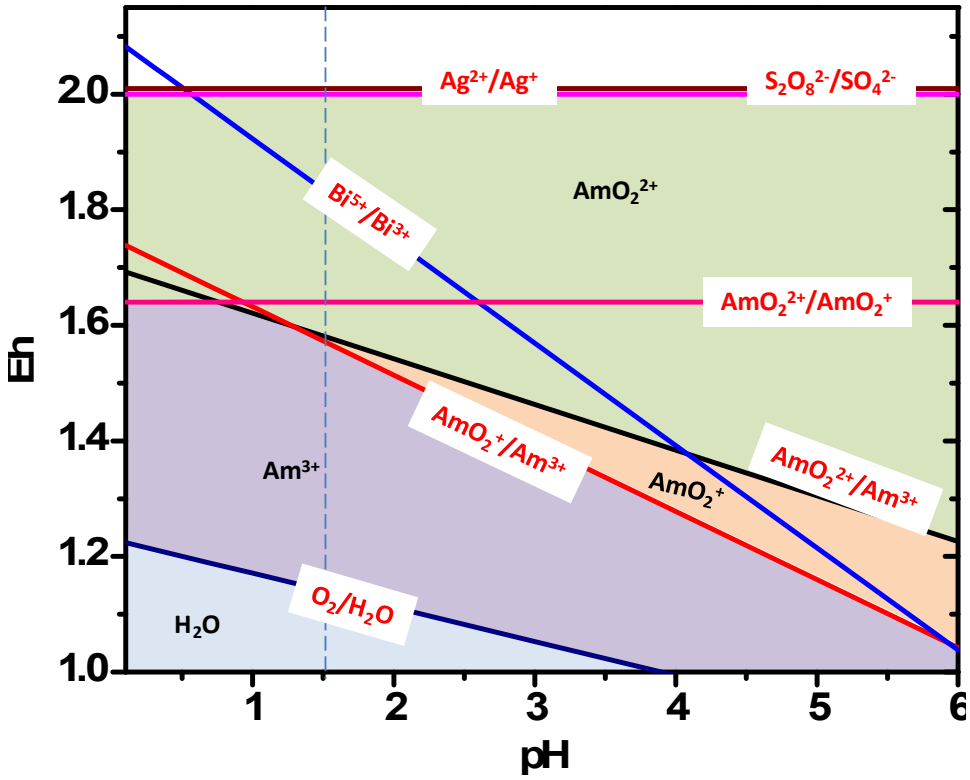

Figure S 3. The Pourbaix diagram of Am-Bi-Ag-S_2O_8 system

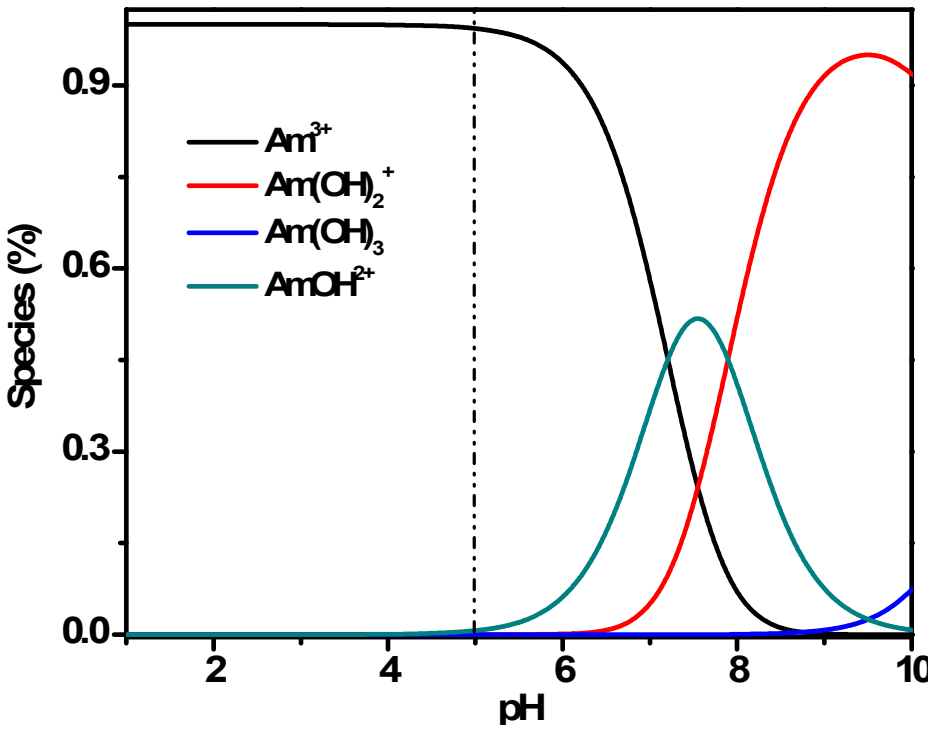

Figure S4. Speciation diagram of Am^{3+} in aqueous media

Table S 2. The thermodynamic equation used to plot Am^{3+} speciation diagram

Thermodynamic equations	**logβ**
$Am^{3+} + H_2O \rightarrow AmOH^{2+} + H^+$	-7.2
$Am^{3+} + H_2O \rightarrow Am(OH)_2^+ + 2\ H^+$	-15.1
$Am^{3+} + H_2O \rightarrow Am(OH)_3 + 3\ H^+$	-26.2
$H_2O \rightarrow H^+ + OH^-$	-14.0

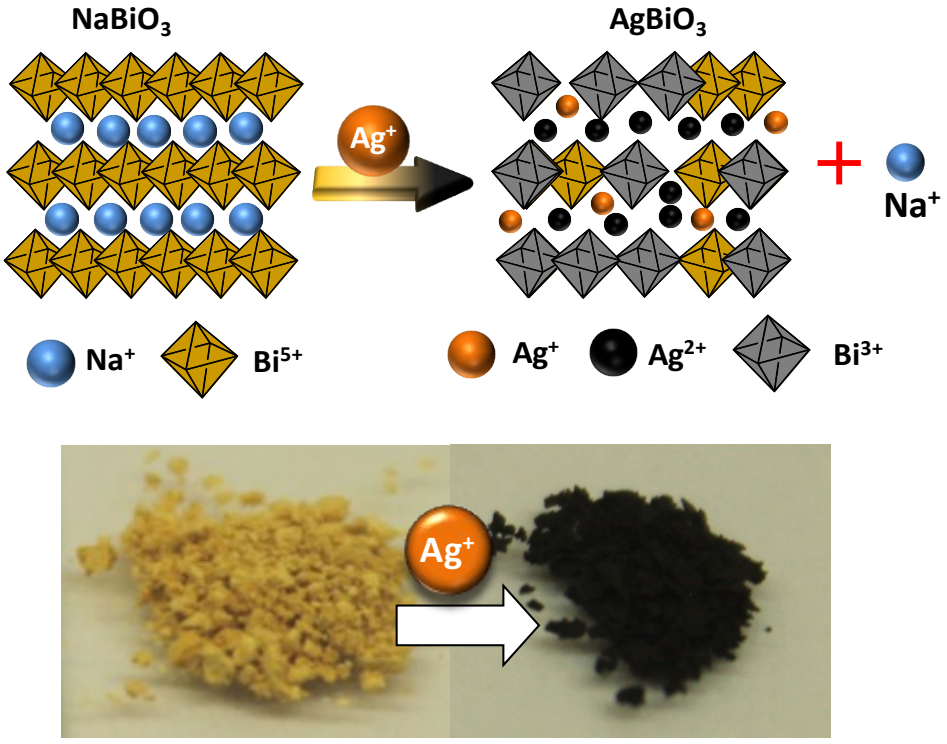

Figure S 5. Synthesis of $AgBiO_3$ by ion-exchange reaction between $NaBiO_3$ and $AgNO_3$ in aqueous medium, Temperature: 298K, Stirring: 60 minutes

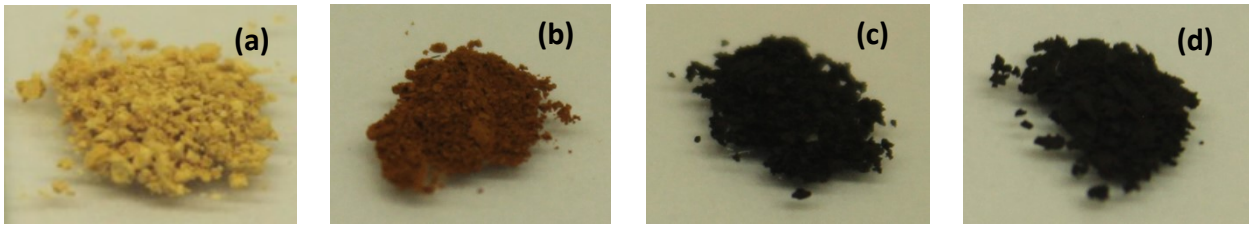

Figure S 6. The photograph of (a) pristine $NaBiO_3$, (b) H^+ activated $NaBiO_3$, and AgBiO3 at (c) 1:1 and (d) 3:1 mole ratio of $AgNO_3$ and $NaBiO_3$.

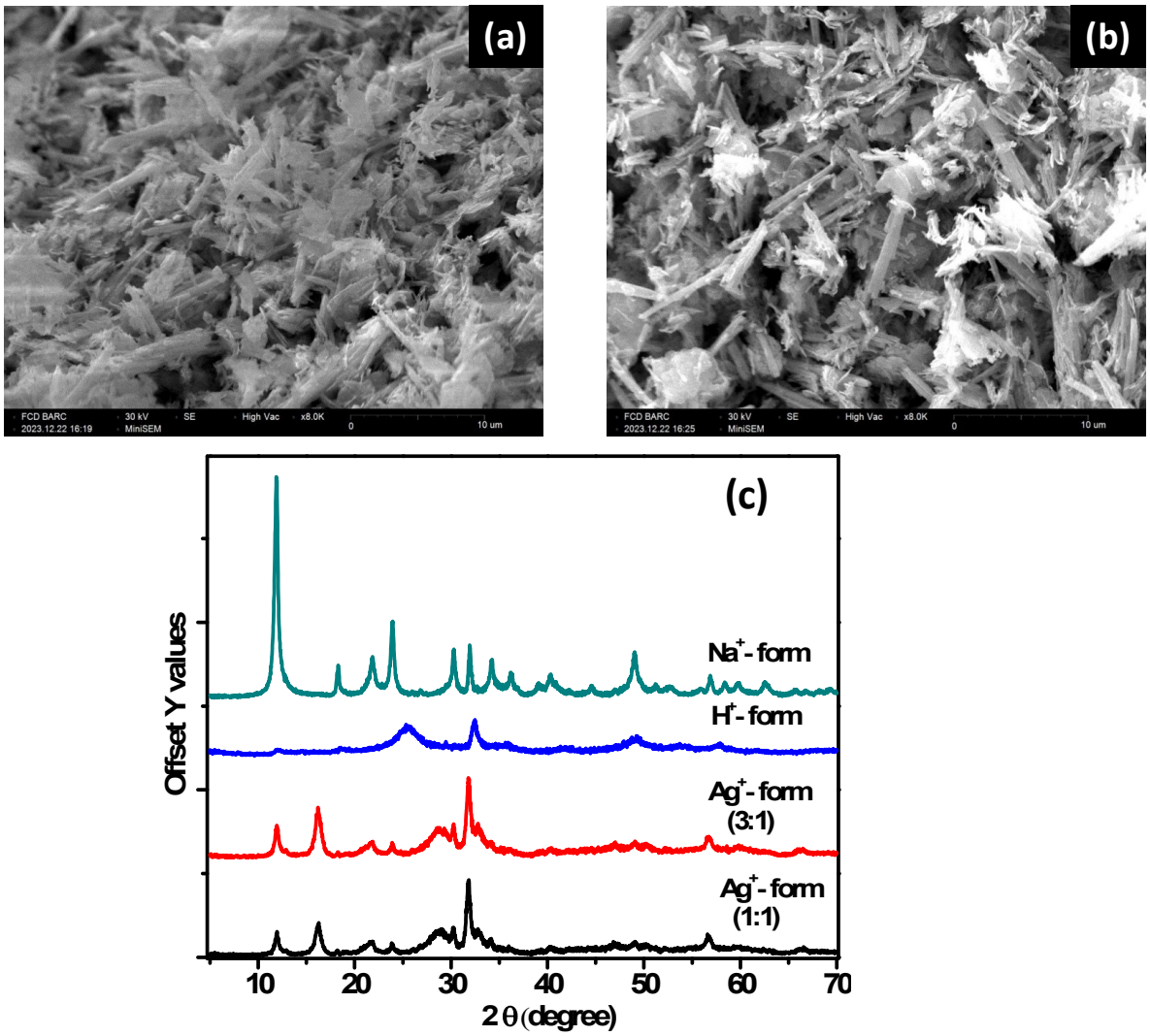

Figure S 7. The SEM images of (a) $NaBiO_3$, (b) $AgBiO_3$, (c) XRD of Na^+, H^+, and Ag^+ form of BiO_3^- at 1:1 and 3:1 $AgNO_3$:$NaBiO_3$ mole ratio.

Table S 3. The % contribution of different forms of Ag and Bi in the $AgBiO_3$

Element	Peak position (eV)	% Contribution (%std Dev)	Nature of species
Ag_3d	368.0	81.7 (0.75%)	Ag^{2+}
	374.0	89.2(0.39%)	
	368.9	18.3 (0.41%)	Ag^{+}
	375.4	10.8 (0.43%)	
Bi_4f	159.0	63.7 (0.29%)	Bi^{3+}
	164.3	63.0 (0.43%)	
	159.9	36.3 (0.26%)	Bi^{5+}
	165.2	37.0 (0.61%)	

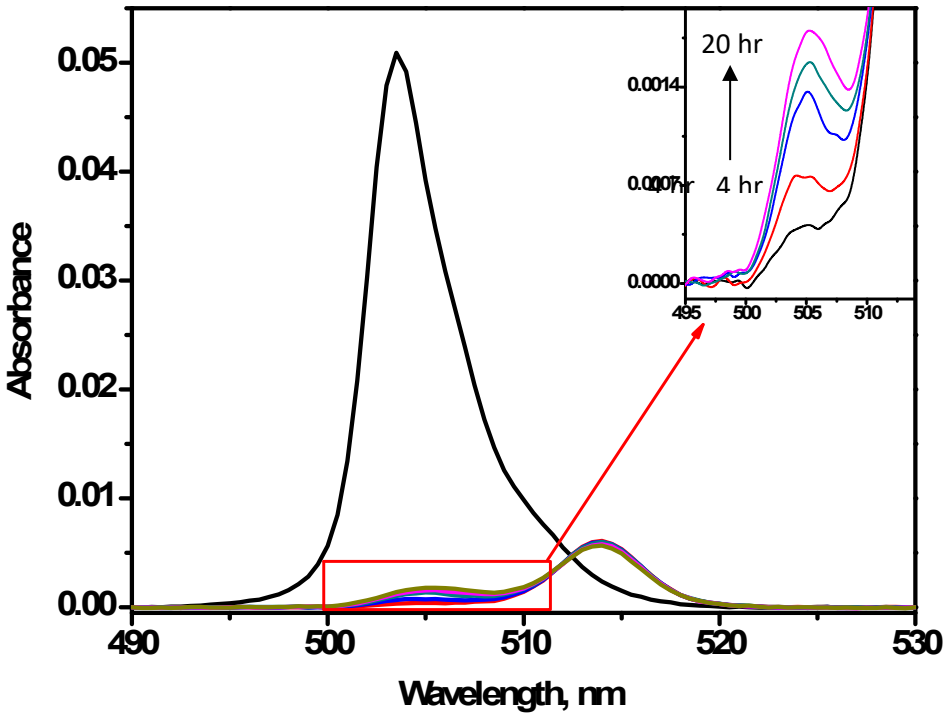

Figure S8. The initial Am^{3+} spectrum (black) and rise in the Am^{3+} peak at 503 nm with time (4 to 20 hr) after quantitative conversion of Am^{3+} to AmO_2^+ on equilibration with $AgBiO_3$, [Am^{3+}]: 1.2×10^{-4} M, [$AgBiO_3$]: 2.5 mg/mL, pH: 4, Temperature: 25 °C.

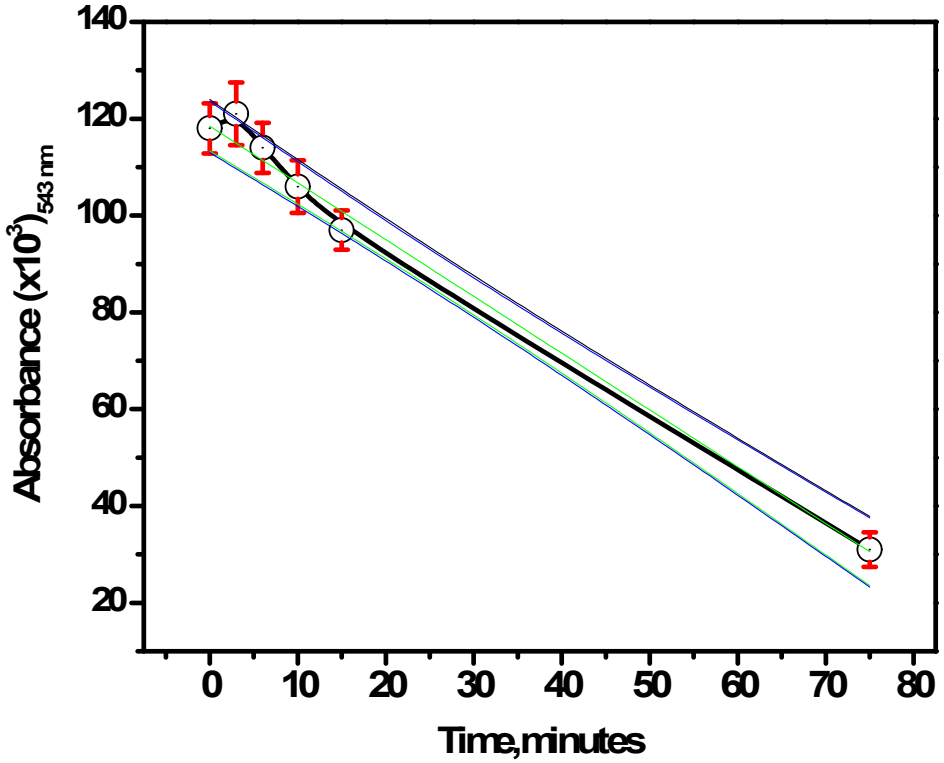

Figure S9. The decrease in the solution concentration of BiO_3^- (estimated using absorbance at 543 nm, (ε: 11.0 reported by Einkauf et al[26]) with time in the supernatant of $AgBiO_3$-Am^{3+}, suspension centrifuged at 10,000 RPM for 10 minutes; [Am^{3+}]: 1.2×10^{-4} M, [$AgBiO_3$]: 2.5 mg/mL, pH: 4, Temperature: 25 °C. The error is shown at the confidence level of 95%.

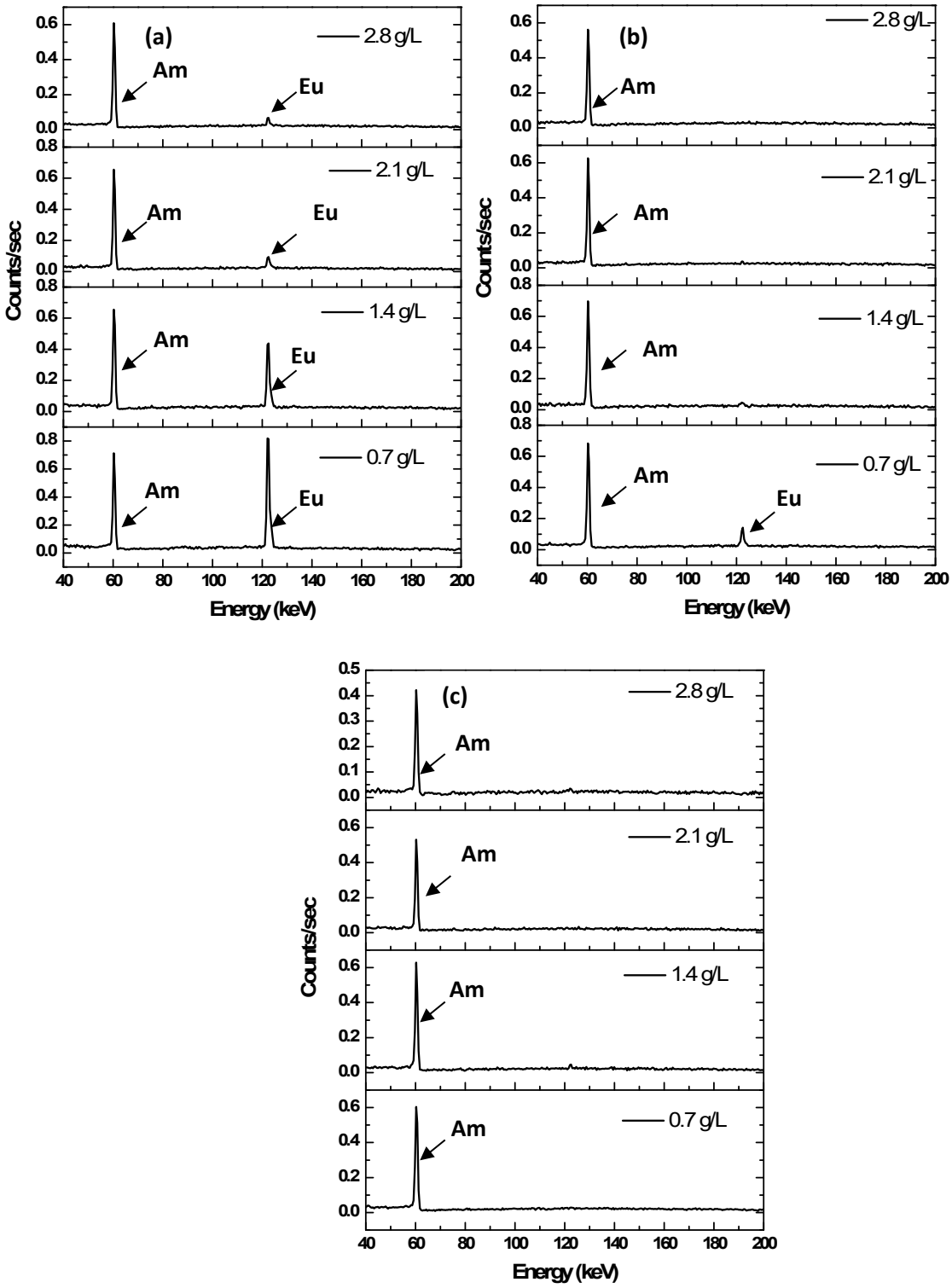

Figure S10. The HpGe spectrum of Am-Eu mixture after contact with different amount of $AgBiO_3$ (0.7, 1.4, 21 and 2.8 g/L) at different time intervals (a) 5 minutes, (b) 30 minutes and (c) 60 minutes, pH: 4, T : 25 °C. (The γ-spectroscopy was performed using HPGe detector.)

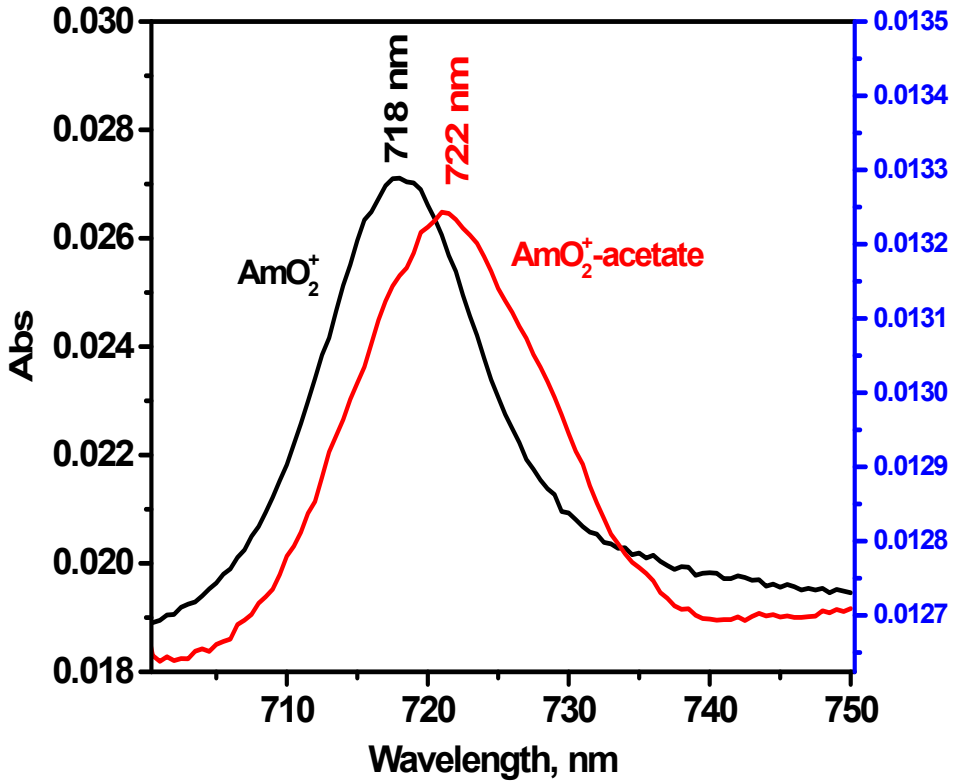

Figure S11. The shift in the AmO_2^+ peak after addition of Na-acetate ion, pH: 4, $[Am^{3+}]$: 1.2×10^{-4} M, [Na-Acetate] = 0.1 M; Temperature: 25 °C.

Table S 4. Comparison of recent methods with the proposed method in present studies

Reagents	Shortcomings	Ref.*
$NaBiO_3$: 15-20 g/L pH: 1, Temp: 80 °C Time:>30 minutes	Higher $NaBiO_3$ dissolution: Bi^{3+} in solution High temperature	9
$Na_2S_2O_8$ + $Ca(OCl)_2$ pH: 1-2, Temp: 80-100 °C Time: 10–45 min	Interfering ions: $S_2O_8^{-}$, SO_4^{2-}, ClO_x, OCl^- In situ gypsum formation High temperature	19
NaBiO3 : 15-20 g/L pH: 1 (HCl) ,Temp: 25 °C Time: 24 hours	Corrosive acid Cl_2 effervescences Insitu BiOCl generation	21
$AgBiO_3$: 2-3 g/L pH: 4, Temp: 25 °C Time: 5-10 minutes	Room temperature, No interfering ions pH ~4: poor disproportionation	p.w.

References

1. J. D. Burns, M. Borkowski, A. Clearfield and D. T. Reed, 2012, **100**, 901-906.
2. Z. Kazi, N. Guérin, M. Christl, M. Totland, A. Gagné and S. Burrell, *J. Radioanal. Nucl. Chem.*, 2019, **321**, 227-233.
3. P. Zsabka, A. Wilden, K. Van Hecke, G. Modolo, M. Verwerft and T. Cardinaels, *J. Nucl. Mater.*, 2023, **581**.
4. J. D. Burns, T. C. Shehee, A. Clearfield and D. T. Hobbs, *Anal. Chem.*, 2012, **84**, 6930-6932.
5. X. Dong, H. Hao, J. Chen, Z. Wang and C. Xu, *Chemical Science*, 2024, **15**, 2118-2122.
6. Z. Wang, J. B. Lu, X. Dong, Q. Yan, X. Feng, H. S. Hu, S. Wang, J. Chen, J. Li and C. Xu, *J. Am. Chem. Soc.*, 2022, **144**, 6383-6389.
7. Z. Wang, X. Dong, Q. Yan, J. Chen and C. Xu, *Anal. Chem.*, 2022, **94**, 7743-7746.
8. W. H. Runde and B. J. Mincher, *Chem. Rev.*, 2011, **111**, 5723-5741.
9. B. J. Mincher, L. R. Martin and N. C. Schmitt, *Inorg. Chem.*, 2008, **47**, 6984-6989.
10. T. S. Grimes, B. J. Mincher and N. C. Schmitt, *Reduction Rates for Higher Americium Oxidation States in Nitric Acid*, Idaho National Lab.(INL), Idaho Falls, ID (United States), 2015.
11. L. B. Asprey, S. E. Stephanou and R. A. Penneman, *J. Am. Chem. Soc.*, 1951, **73**, 5715-5717.
12. K. McCann, D. M. Brigham, S. Morrison and J. C. Braley, *Inorg. Chem.*, 2016, **55**, 11971-11978.
13. B. J. Mincher, L. R. Martin and N. C. Schmitt, 2007.
14. J. S. Coleman, T. K. Keenan, L. H. Jones, W. T. Carnall and R. A. Penneman, *Inorg. Chem.*, 1963, **2**, 58-61.
15. L. B. Asprey, S. E. Stephanou and R. A. Penneman, *J. Am. Chem. Soc.*, 1950, **72**, 1425-1426.
16. L. B. Werner and I. Perlman, *J. Am. Chem. Soc.*, 1951, **73**, 495-496.
17. G. P. Horne, T. S. Grimes, W. F. Bauer, C. J. Dares, S. M. Pimblott, S. P. Mezyk and B. J. Mincher, *Inorg. Chem.*, 2019, **58**, 8551-8559.
18. T. S. Grimes, G. P. Horne, C. J. Dares, S. M. Pimblott, S. P. Mezyk and B. J. Mincher, *Inorg. Chem.*, 2017, **56**, 8295-8301.
19. B. J. Mincher, N. C. Schmitt, B. K. Schuetz, T. C. Shehee and D. T. Hobbs, *RSC Adv.*, 2015, **5**, 27205-27210.
20. J. P. Nigon, R. A. Penneman, E. Staritzky, T. K. Keenan and L. B. Asprey, *The Journal of Physical Chemistry*, 1954, **58**, 403-404.
21. N. T. Rice, E. Dalodière, S. L. Adelman, Z. R. Jones, S. A. Kozimor, V. Mocko, H. D. Root and B. W. Stein, *Inorg. Chem.*, 2022, **61**, 12948-12953.
22. W. Dou, X. Hu, L. Kong, X. Peng and X. Wang, *Desalination*, 2020, **491**.
23. Y. Feng, X. Huang, Q. Zhan and D. Jiang, *Journal of Materials Science: Materials in Electronics*, 2019, **30**, 10543-10549.
24. S. Ahrland, J. O. Liljenzin and J. Rydberg, in *Comprehensive Inorganic Chemistry*, eds. J. C. Bailar, H. J. Emeleus, R. Nyholm and A. F. Trotman-Dickenson, Pergamon, Oxford, 1973, DOI: https://doi.org/10.1016/B978-1-4832-8313-5.50033-4, pp. 465-635.
25. M. H. Ford-Smith and J. J. Habeeb, *J. Chem. Soc., Dalton Trans.*, 1973, DOI: 10.1039/DT9730000461, 461-464.
26. J. D. Einkauf and J. D. Burns, *ACS Applied Energy Materials*, 2020, **3**, 1593-1601.